Clinica Chimica Acta 481 (2018) 25–33

Contents lists available at ScienceDirect

Clinica Chimica Acta

journal homepage: www.elsevier.com/locate/cca

Functional and pharmacological evaluation of novel *GLA* variants in Fabry disease identifies six (two *de novo*) causative mutations and two amenable variants to the chaperone DGJ

Lorenzo Ferri[a], Duccio Malesci[b], Antonella Fioravanti[c], Gaia Bagordo[b], Armando Filippini[d], Anna Ficcadenti[e], Raffaele Manna[f], Daniela Antuzzi[f], Elena Verrecchia[f], Ilaria Donati[g], Renzo Mignani[h], Catia Cavicchi[a], Renzo Guerrini[a,b], Amelia Morrone[a,b,*]

[a] *Paediatric Neurology Unit and Laboratories, Meyer Children's Hospital, Firenze, Italy*
[b] *Department of NEUROFARBA, University of Florence, Firenze, Italy*
[c] *Structural Biology Researcher Center, VIB, Vrije Universiteit Brussel, Brussels, Belgium*
[d] *Nephrology and Dialysis Unit, Ospedale Policlinico Casilino, Roma, Italy*
[e] *Institute of Maternal-Infant Sciences, Politecnico Universitario delle Marche, Ancona, Italy*
[f] *Gemelli Policlinic, Catholic University of Sacred Heart, Rome, Italy*
[g] *Medical Genetics Unit, AUSL di Romagna, Cesena, Italy*
[h] *Nefrology Unit, Ospedale degli Infermi, Rimini, Italy*

ARTICLE INFO

Keywords:
1-Deoxygalactonojirimycin
DGJ
De novo mutation
Atypical variants
Lipofectamine
Site-directed mutagenesis

ABSTRACT

Background: Allelic heterogeneity is an important feature of the *GLA* gene for which almost 900 known genetic variants have been discovered so far. Pathogenetic *GLA* variants cause alpha-galactosidase A (α-Gal A) enzyme deficiency leading to the X-linked lysosomal storage disorder Fabry disease (FD). Benign *GLA* intronic and exonic variants (*e.g.* pseudodeficient p.Asp313Tyr) have also been described. Some *GLA* missense variants, previously deemed to be pathogenetic (*e.g.* p.Glu66Gln and p.Arg118Cys), they have been reclassified as benign after re-evaluation by functional and population studies. Hence, the functional role of novel *GLA* variants should be investigated to assess their clinical relevance.

Results: We identified six *GLA* variants in 4 males and 2 females who exhibited symptoms of FD: c.159C > G p.(Asn53Lys), c.400T > C p.(Tyr134His), c.680G > C (p.Arg227Pro), c.815A > T p.(Asn272Ile), c.907A > T p.(Ile303Phe) and c.1163_1165delTCC (p.Leu388del). We evaluated their impact on the α-Gal A protein by bioinformatic analysis and homology modelling, by analysis of the *GLA* mRNA, and by site-directed mutagenesis and *in vitro* expression studies. We also measured their responsiveness to the pharmacological chaperone DGJ.

Conclusions: The six detected *GLA* variants cause deficient α-Gal A activity and impairment or loss of the protein wild-type structure. We found p.Asn53Lys and p.Ile303Phe variants to be susceptible to DGJ.

1. Introduction

Allelic heterogeneity is a predominant feature of the *GLA* gene (located at position Xq22.1, OMIM 300644, RefSeq X14448) which counts 900 known variants (Human Gene Mutation Database Professional, www.biobase-international.com) in a protein of 429 amino acids: the lysosomal α-galactosidase A (α-Gal A; EC 3.2.1.22). Pathogenetic variants of the *GLA* gene cause total or partial α-Gal A enzyme deficiency and induce the progressive development of the X-linked lysosomal storage disorder, Fabry disease (FD; OMIM 301500) [1]. The α-Gal A enzyme catalyses the hydrolysis of α-galactosidic linkages of glycosphingolipids, glycoproteins and polysaccharides [1]. Deficiency of α-Gal A enzyme activity induces accumulation of glycosphingolipids containing terminal α-galactose residues within the lysosomes of many tissues, including the kidney, arteries and heart [1,2].

Laboratory confirmation of FD in males relies on the demonstration of deficient α-Gal A activity in leukocytes or fibroblasts followed by *GLA* gene sequencing. Milder forms of FD are usually associated with residual enzyme activity. Heterozygous females may develop mild to severe clinical manifestations [1,3], but enzyme assay is unreliable in females due to random X-chromosome inactivation. Hence, *GLA* gene sequencing is crucial for confirming FD in females.

Abbreviations: α-Gal A, alpha-galactosidase A; FD, Fabry disease; DGJ, 1-deoxygalactonojirimycin; VUS, variants of unknown significance

* Corresponding author at: Molecular and Cell Biology Laboratory, Paediatric Neurology Unit and Laboratories, Meyer Children's Hospital, Viale Pieraccini n. 24, 50139 Firenze, Italy.
E-mail address: a.morrone@meyer.it (A. Morrone).

https://doi.org/10.1016/j.cca.2018.02.021
Received 22 January 2018; Received in revised form 24 January 2018; Accepted 19 February 2018
Available online 21 February 2018
0009-8981/

FD is characterized by a heterogeneous spectrum of clinical manifestations [1,2] and most of the signs and symptoms resemble those of other common diseases. Several FD forms have been recognized, ranging from a milder condition with only cardiac and/or renal abnormalities, to the more classic FD phenotype characterized by chronic pain, vascular degeneration, angiokeratoma, cardiac abnormalities, kidney manifestations leading to renal failure, and other symptoms [1,2]. Establishing a correlation between *GLA* nucleotide variants and patients' phenotypes can represent a challenge. Some missense *GLA* variants have been reported in clinical case reports which lack functional assessment. Other missense *GLA* variants, which as yet lack correlation with a phenotype, have been reported in newborns through newborn screening programs.

Besides the pathogenetic variants, several intronic polymorphic variants and one missense change (*i.e.* p.Asp313Thr) which is responsible for a pseudodeficiency have also been described [4–7]. Pseudodeficiency variants cause false positives in the enzyme assay but are not disease causing. Some *GLA* missense variants (p.Pro60Leu, p.Glu66Gln, p.Arg118Cys, p.Ala143Thr, p.Ile198Thr; aliases p.P60L, p.E66Q, p.R118C, p.A143T and p.I198T) that had been reported as causative when first discovered, have resulted as benign polymorphisms in subsequent clinical, functional and population studies [4,8–11]. Such findings stress the importance of performing exhaustive assessments of the effects of new *GLA* VUS when detected in patients with suspected FD.

Such a high allelic heterogeneity makes the identification of *GLA* variants of unknown significance (VUS) in routine molecular confirmation for FD quite frequent. VUS produce uncertainty both for those responsible for giving a laboratory report, and for clinicians managing a patient. They increase the risk of misdiagnosis, especially if the patient does not exhibit obvious signs of classic FD [12]. Early diagnosis of FD in affected patients is of great importance since a specific enzyme replacement therapy (ERT) [12] is available. A clear-cut exclusion of FD in suspected patients is of equal importance to avoid distress in families and inappropriate initiation of ERT, which is invasive and extremely expensive [12].

Besides ERT, a new alternative treatment option based on the small-molecule pharmacological chaperone 1-deoxygalactonojirimycin (or DGJ) is available [13]. DGJ reversibly binds to the active site of α-Gal A and stabilises the 3D structure of mutant forms of the enzyme which are affected by conformational mutations, rescuing enzyme activity [13–18]. Responsiveness to this therapeutic option can be tested by administering DGJ to cell lines expressing mutant forms of α-Gal A and by measuring the rescue of the α-Gal A enzyme activity [5,19].

Hence, performing functional and pharmacological studies of novel *GLA* variants can be twofold helpful in assessing their clinical significance and deciding which therapeutic options are likely to be effective. Such studies can be performed *in vitro* on cell lines transfected with mutated vectors or directly on patients' derived cell lines, when available [5].

Here we report the clinical, functional and pharmacological characterization of six new *GLA* gene variants found in patients with symptoms on the FD clinical spectrum. We performed *in vitro* expression studies and studies on patients' derived cells to evaluate impact on the α-Gal A activity and on the α-Gal A protein and to estimate responsiveness to DGJ.

2. Materials and methods

2.1. Patients

Patients' clinical data and α-Gal A activities are reported in Table 1. Whole blood DNA samples from patients and their relatives were examined after informed consent was obtained for all individuals, in accordance with local ethical committee recommendations. The family pedigrees are shown in Fig. 1.

2.2. Analysis of genomic DNA

Genomic DNA was isolated using the QIAsymphony DSP DNA Midi Kit and the QIAsymphony robot (Qiagen, Hilden, Germany).

The entire coding region with intron-exon boundaries and a region of the intron IV which includes the NM_000169.2:c.639 + 861C > T [20] and NM_000169.2:c.639 + 919G > A [21] deep intronic mutations were amplified and sequenced using previously published oligonucleotides and reaction conditions [22].

Two allelic dosage assays, MLPA (Multiplex Ligation-dependent Probe Amplification) and Quantitative Fluorescent Multiplex PCR (QFM-PCR) [22], were both applied on DNA samples from the two female FD patients (Pt1 and Pt4) in order to exclude gross *GLA* gene rearrangements [22].

2.3. Bioinformatics analysis

The identified *GLA* variants were analysed in the HGMD professional database (http://www.biobase-international.com/product/hgmd), dbSNP database (http://www.ncbi.nlm.nih.gov/snp), ExAC browser (http://exac.broadinstitute.org) and 1000 genomes project browser (http://browser.1000genomes.org/index.html).

We used Alamut Visual (http://www.interactive-biosoftware.com) to predict the possible pathogenicity of the identified *GLA* variants. The Alamut software integrates 4 different prediction tools for missense changes: Mutation Taster (http://www.mutationtaster.org), PolyPhen-2 (http://genetics.bwh.harvard.edu/pph2), SIFT (http://sift.bii.a-star.edu.sg) and Align GVGD (http://agvgd.iarc.fr). Alamut also provides phylogenetic conservation data of interrogated protein amino acid residues.

Possible alterations in *GLA* mRNA splicing processing were also checked by Alamut Visual which integrates 5 different specific algorithms (SpliceSiteFinder, MaxEntScan, NNSPLICE, GeneSplicer, Human Splicing Finder) predicting if a given variant impairs mRNA splicing.

2.4. Site-directed mutagenesis

We generated mutant plasmid to express the p.Asn53Lys, p.Tyr134His, p.Arg227Pro, p.Asn272Ile, p.Ile303Phe variants using PCR-based site-directed mutagenesis of *GLA* cDNA, cloned into the expression vector pCD-X, as previously described [23]. Forward primers: 5′-TTCATGTGCAAGCTTGACT GCCAG-3′ (p.Asn53Lys), 5′-CTAGGGATTCATGCAGATGT-3′ (p.Tyr134His), 5′-AATCACTGGCCAAATTTTGCTG-3′ (p.Arg227Pro), 5′-GTGATTGGCATCT TTGGCCTC-3′ (p.Asn272Ile) and 5′-CCTCCGACACTTCAGCCCTCAA-3′ (p.Ile303Phe) and reverse primers: 5′-CTGGCAGTCAAGCTTGCACATGAA-3′ (p.Asn53Lys), 5′-ACATCTGCATGAATCCCTAG-3′ (p.Tyr134His), 5′-CAGCAA AATTTGGCCAGTGATT-3′ (p.Arg227Pro), 5′-GAGGCCAAAGATGCCAAT CAC-3′ (p.Asn272Ile) and 5′-TTGAGGGCTGAAGTGTCGGAGG-3′ (p.Ile303Phe) were used for the mutagenesis reactions according to the standard protocols. For the construction of the plasmid carrying the p.Leu388del variant, we amplified a DNA fragment containing this variant directly from the Pt6's DNA using forward primer 5′-GGAGACAACTTTGAA GTGTG-3′ and reverse primer 5′-CCGAATTCTTAAAGTAAGTCTTTTAA-3′, both annealing to *GLA* exon 7. All the PCR amplifications were performed with FastStart High Fidelity PCR System (Hoffmann-La Roche, Basilea, Switzerland). Ligations were carried out using Solution I of the DNA Ligation Kit Ver.2.1 (TaKaRa Bio Inc., Kusatsu, Japan). *Escherichia coli* strain Solo pack gold cells (Stratagene, Milan, Italy) were used for cloning. We confirmed the mutated plasmid constructs obtained by sequencing the full-length *GLA* cDNA. We prepared large-scale plasmid preparations using the EndoFree Plasmid Maxi Kit (Qiagen, Hilden, Germany).

2.5. COS-1 cell transfection and effect of DGJ on α-Gal A activity

We transiently overexpressed normal and mutant plasmids pCD-Asn53Lys, pCD-Tyr134His, pCD-Arg227Pro, pCD-Asn272Ile, pCD-Ile303Phe and pCD-Leu388del into African green monkey kidney cells (COS-1). COS-1 cells were grown at 37 °C, 5% CO_2 in DMEM (Dulbecco's modified Eagle medium) (1:1 vol/vol) with fetal bovine

Table 1
Patient's data.

	Pt1	Pt2	Pt2's mother	Pt3	Pt3's mother	Pt3's sister	Pt4	Pt5	Pt6
Sex	Female	Male	Female	Male	Female	Female	Female	Male	Male
Age at diagnosis (y)	70	46	76	38	62	35	nd	38	11
Age at present (y)	43	35	65	35	59	32	nd	35	13
Angiokeratoma	−	+	−	+	+	+	−	−	−
Musculoskeletal and bone manifestations	−	−	+	−	−	−	−	−	−
Cornea verticillata	−	−	−	+	+	−	−	−	−
Abdominal pain	−	−	−	+	+	−	−	+	+
Diarrhea/ constipation	−	−	−	−	−	−	−	+	+
Tinnitus and/or hearing loss	−	+	−	−	−	−	−	+	−
Vertigo	−	−	−	−	+	−	−	+	−
Acroparesthesias	−	−	−	+	+	−	+	+	−
Fever pain crisis	−	+	−	+	−	−	−	+	+
Cardiovascular manifestations	−	+	+	+	+	−	−	−	−
Cardiomyopathy	−	+	−	+	+	−	+	+	−
Cerebrovascular manifestations	−	+	−	+	+	−	−	+	−
Valve disease	+	+	−	+	−	−	−	−	−
ECG abnormalities	−	+	+	+	+	−	−	+	−
Hypertension	+	+	+	−	+	−	−	−	−
Renal manifestations	+	+	−	+	−	−	+	−	−
Other	−	HCV; renal transplantation in 1997	−	−	Hypothyroidism	−	−	−	−
α-GAL A activity (n.v. > 20 nmol/mg/h)	53	0	37	0	28	26,2	−	4,5	0
GLA variant	c.159C > G p.(Asn53Lys)	c.400T > C p.(Tyr134His)	c.400T > C p.(Tyr134His)	c.680G > C p.(Arg227Pro)	c.680G > C p.(Arg227Pro)	c.680G > C p.(Arg227Pro)	c.815A > T p.(Asn272Ile)	c.907A > T p.(Ile303Phe)	c.1163_1165delTCC p.(Leu388del)

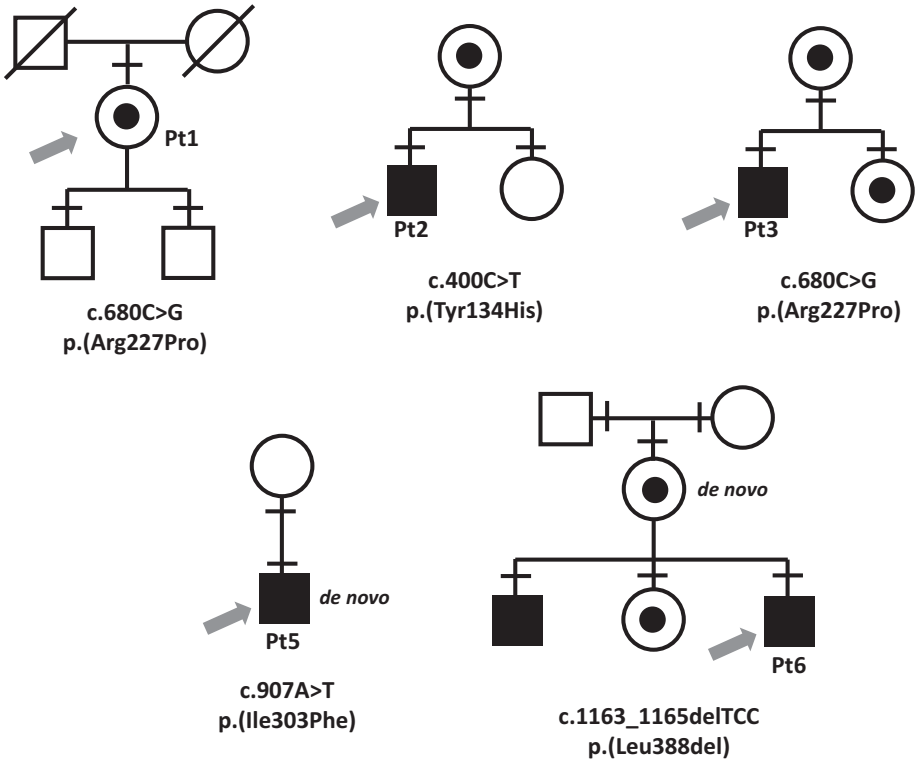

Fig. 1. Pedigree charts of Fabry patients.

serum (FBS, 10%) and antibiotics (Penicillin-Streptomycin 1 ×). Before transfection, COS-1 cells were seeded in 6-well plates at a density of 7.5×10^5 cells/well in DMEM without fetal bovine serum and antibiotics and were incubated at 37 °C, 5% CO_2 for 2 h. Cell transfections were mediated by Lipofectamine 2000 (Life Technologies, Carlsbad, CA, USA) using a plasmid DNA/lipofectamine ratio of 1 μg:2.5 μl. We used an amount of 2.5 μg of plasmid DNA for each transfection sample. After transfection, we incubated the cells at 37 °C, 5% CO_2 for 2 h before adding fresh DMEM medium (with FBS and antibiotics) alone or with 20 μM (final concentration) DGJ (1-deoxygalactonojirimycin; migalastat; Sigma-Aldrich), which is the optimal concentration for many other mutant forms of α-Gal A [19,23,24]. We incubated the cells for 48 h before harvesting by trypsinization. After trypsinization, we washed the cells once with PBS and we re-suspended the pellet in distilled water supplemented with a protease inhibitor (Sigma-Aldrich, St. Louis, MO, USA) in accordance with the manufacturer's instructions. Pellets were stored at −20 °C.

2.6. T cell-based assays

We performed T cell-based assays by incubating patients' derived cultured T-lymphocytes with 0 or 20 μM DGJ for 5 days at 37 °C in 5% CO_2. After incubation, cells were harvested and washed four times with 1 ml physiological solution. Lymphocyte pellets were lysed by sonication for 10 s and tested in triplicate by α-Gal A enzyme assay, as below.

2.7. α-Gal A enzyme assay

We performed α-GAL A enzyme assays in triplicate by fluorogenic method [23] with the following modifications: 1 mg/ml cell lysates (diluted in 10 μl of heat inactivated 0.2% BSA + 0.02% Na Azide) were added to 20 μl substrate (4-MU-a-D-galactopyranoside 5 mM in 0.1 M Na-acetate buffer, pH 4.5 + 150 mM *N*-acetyl-D-galactosamine and 0.02% Na Azide); stop solution: 200 μl of 0.5 M Na-HCO_3-Na_2Co_3 buffer, pH 10.7, 0.025% Triton X-100. The Micro BCA protein Assay kit (Pierce Rockford, IL, USA) was used to set up the starting protein concentrations used in each enzyme assay performed in black 96-well microplates. Fluorescence was read on a Spectra Max M2 microplate Reader (Molecular Devices, Toronto, Canada).

2.8. Western blot analysis

We performed western blot analysis by loading 30 μg of total lysates (lymphocytes lysed by sonication) per well. We prepared blots from 12.5% polyacrylamide gels and probed as previously described [25]. After electrophoresis, we transferred proteins onto nitrocellulose (Bio-Rad, Hercules, CA, USA) and the filters were incubated with anti-α-Gal A antibodies kindly provided by Genzyme Italia (Genzyme, Modena, Italy). We incubated the blots with a secondary anti-rabbit IgG (whole molecule) conjugated to alkaline phosphatase (SIGMA, Milano, Italy), and we revealed signals using the AP Conjugate Substrate kit (Bio-Rad, Hercules, CA).

2.9. RNA isolation, reverse-transcriptase PCR (RT-PCR) and cDNA analysis

We isolated total RNA from patients' derived cultured T-lymphocytes and four controls using the RNeasy mini kit (Qiagen, Hilden Germany). Patients Pt1 and Pt6 gave the consent for this analysis. RNA integrity and concentration were both checked by 1% agarose gel and Nanodrop ND-1000 Spectrophotometer (Nanodrop technologies, Wilmington, USA). We retrotranscribed total RNAs (200 ng) with random hexamers, oligo-dT primers and a specific oligo (GLA-RNA7R 5′-GTCTTTTAATGACATCTGCAT-3′) annealing to *GLA* exon 7, using Takman Reverse Transcription kit (Applied Biosystems-Thermo Fisher Scientific, Carlsbad, CA, USA) in accordance with the manufacturer instructions. We performed PCR amplifications using 2 μl of RT-PCR products as template: for patient 1, we used forward primer GLA-RNA1F 5′-TTCATGTGCAACCTTGACTGC-3′, which anneals in the *GLA* exon 1, and reverse primer GLA-RNA3R, annealing to the *GLA* exon 3; for patient 6, we combined forward primers GLA-RNA1F and GLA-RNA5F 5′-CTGGCGAAATTTTGCTGACA-3′, annealing to the *GLA* exon 5 with the reverse primer GLA-RNA7R. PCR products were checked by 1% agarose gel electrophoresis.

2.10. Homology modelling

The crystal structures of the α-GAL mature human form are available in complex with its ligand galactose [26,27]. We made the homology models of the new gene variants described in this study using SWISS MODEL (http://swissmodel.expasy.org) in order to map the missense variants to the three-dimensional structure wild-type template and better comprehend their effect on the protein structure-function. The p.(Asn53Lys), p.(Tyr134His), p.(Arg227Pro), p.(Asn272Ile), p.(Ile303Phe) and (p.Leu388del) α-Gal amino acid sequences were used as targets for the Homology Modelling (HM) analysis and the α-Gal structure as template (Protein Data Bank accession code 3s5z [27]). We super-imposed the PDB files generated by HM with the wild-type structure of the α-Gal with bound α-galactose by PyMOL software (The PyMOL Molecular Graphics System, Version 0.99, DeLano Scientific, LLC, San Carlos, CA).

2.11. GLA gene variants nomenclature and reference sequence

GLA gene variants are given in the text by following the HGVS recommendations (http://www.hgvs.org/mutnomen/). *GLA* gene variants were submitted to the LOVD database (http://grenada.lumc.nl/LOVD2/MR/home.php?select_db=GLA). Exon numbering refers to refseq NM_000169.2 (*GLA*; Gene ID 2717 in http://www.ncbi.nlm.nih.gov/gene/).

3. Results

3.1. Identification of GLA gene variants in probands with FD manifestations

We measured α-Gal A enzyme activity and sequenced the *GLA* gene in 2 females and 4 males with clinical manifestations on the FD clinical spectrum (Table 1). We detected a deficiency in α-Gal A activity in males while females exhibited normal values (Table 1). By *GLA* sequencing, we identified six previously uncharacterized gene variants. Five variants were missense changes: c.159C > G p.(Asn53Lys), c.400T > C p.(Tyr134His), c.680G > C p.(Arg227Pro), c.815A > T p.(Asn272Ile) and c.907A > T p.(Ile303Phe). One additional variant was an in-frame trinucleotide deletion, the c.1163_1165delTCC, which leads to an in-frame single amino acid deletion at the protein level (p.Leu388del). These *GLA* variants are novel with the exception of the c.680G > C p.(Arg227Pro) [28].

We also performed *GLA* allele dosage in the two females by MLPA and QFM-PCR [22] excluding gross *GLA* gene rearrangements in their genome.

3.2. Screening of at risk family members

An analysis of at risk family members identified six additional subjects carrying *GLA* gene variants, 5 females and 1 male (Fig. 1). We found that two *GLA* variants (the c.907A > T and c.1163_1165delTCC) originated by *de novo* mutational events in two families (Pt5 and in Pt6, Fig. 1).

3.3. In silico analysis of GLA missense variants

Five *GLA* variants are not reported in the HGMD professional

database or in the dbSNP database, while the p.Arg227Pro variant has recently been reported in a large Italian family in association with the classic FD phenotype [28]. Analysed variants were also absent in ExAC browser, in 1000 genome browser and in a sample of more than one hundred healthy male controls with normal α-Gal A activity which we had previously analysed and reported [5].

The amino acid substitutions p.Tyr134His, p.Arg227Pro and p.Asn272Ile were concordantly predicted to be pathogenetic by Mutation Taster, PolyPhen-2, SIFT and Align GVGD. The p.Asn53Lys variant was predicted to be deleterious by Mutation Taster and PolyPhen-2, while SIFT and Align GVGD predicted it to be tolerated. Variant p.Ile303Phe was predicted to be deleterious by Mutation Taster, PolyPhen-2 and SIFT while Align GVGD predicted it to be tolerated.

None of these four missense variants were predicted to cause splicing perturbations, with the exception of the c.159C > G p.(Asn53Lys) nucleotide change which was predicted to abolish an SF2/ASF ESE motif.

The deletion p.Leu388del was not examined by Mutation Taster, PolyPhen-2, SIFT and Align GVGD because these tools are limited to the analysis of missense changes. Alamut Visual predicted a possible alteration of the mRNA splicing due to this variant.

Neither the c.159C > G p.(Asn53Lys) nor the c.1163_1165delTCC p.(Leu388del) are close to exon boundaries, so it was surprising that they were predicted to be splice variants. For this reason, we performed an experimental evaluation (Section 3.4).

3.4. Analysis of GLA mRNA splicing in Pt1 and Pt6

In order to evaluate the splicing predictions obtained by Alamut Visual for the c.159C > G p.(Asn53Lys) and c.1163_1165delTCC p.(Leu388del) variants, we cultivated lymphocytes from Pt1 and Pt6 and analysed the *GLA* mRNA on patients' derived cells. Our analysis did not reveal any aberrant *GLA* transcript in either patient, but confirmed the presence of the c.159C > G p.Asn53Lys and c.1163_1165delTCC p.Leu388del nucleotide variant in their *GLA* mRNA, respectively. These results led us to investigate the impact of these mutations at the protein level.

3.5. Structural analysis by homology modelling

A previous X-ray crystallographic study revealed that the human mature α-Gal A structure corresponds to a homodimeric glycoprotein [26]. Each monomer is composed of two domains: a domain 1 (D1), that contains the active site at the centre of the β strands in the $(\beta/\alpha)_8$ barrel and a C-terminal domain 2 (D2), that contains antiparallel β strands (Fig. 2A).

Using as template the human wild-type (wt) α-galactose-bounded α-Gal A structure [27], we obtained by homology modelling (HM) six models corresponding to the six variant forms of the protein object of this study. We compared those to the wt protein structure in order to map the variants along the 3-D structure of the protein and evaluate their role in structure/function.

Five (Asn53Lys, Tyr134His, Arg227Pro, Asn272Ile and Ile303Phe) out of the six missense changes are localized in the D1 of the protein while the single-amino acid deletion (Leu388del) affects the α-Gal A D2. (Fig. 2).

Both Tyr134His and Arg227Pro missense variants affect the active site of the protein. The p.Tyr134His variant leads to the substitution of a neutral, polar and aromatic residue with a polar and basic amino acid residue, while the p.Arg227Pro variant substitutes a polar with non-polar amino acid residue. The wt α-Gal A active site is composed of 15 side-chains that interact with the ligand α-galactose, 12 of which are extremely conserved across the α-Gal/α-NAGA family [26]. The p.Tyr134His and p.Arg227Pro variants belong to the conserved group of residues. In the wild-type protein Tyr134 and Arg227 are localized in the β3 and β5 strands, respectively, that form the $(\beta/\alpha)_8$ barrel which contains the catalytic site of the α-Gal A. Both residues are involved in the formation of two hydrogen bonds with the α-galactose [26]. These bonds in the mutant forms are not properly formed due to the nature of the substituted residues (p.Tyr134His, p.Arg227Pro) (Fig. 2), possibly explaining the loss of enzyme function observed.

The missense variants p.Asn53Lys and p.Ile303Phe occur in loop regions that are exposed on the surface of the protein. More precisely, the p.Asn53Lys is localized in the α1-α1′ loop at the N-terminal of the D1, while the p.Ile303Phe occurs in the β8-α8 loop region of the same domain. In the case of p.Asn53Lys, a polar non charged residue is substituted by a positively charged residue, while for the p.Ile303Phe both the residues are hydrophobic but one is aliphatic and the other aromatic. The HM revealed that both substitutions can destabilize the α-Gal A 3-D structure despite the fact that they do not dramatically affect the catalytically active site.

The Asn272Ile variant is also localized in a loop region (β7-α7), but buried in the dimerization interface of the protein. The residue is localized beyond the well-conserved Phe273 residue, which is essential for protein dimerization in different species [26]. With this variant a polar uncharged residue is substituted by a hydrophobic one. Even if HM did not detect any secondary structural change due to this substitution, the Asn272Ile could still have an impact by preventing the formation of the homodimer.

The p.Leu388del is the only mutation in this study that affects the D2 of the protein. HM analysis showed a severe structural effect for this mutation (Fig. 2B). This single-amino acid deletion causes the loss of three antiparallel β strands (β 14, β 15 and β 16) resulting in a destruction of the D2 domain and misfolding of the last C-terminal forty-one residues.

3.6. In vitro expression of mutant α-Gal A and response to the pharmacological chaperone DGJ

We transfected the wild-type and mutant forms of *GLA* cDNA in COS-1 cells and we tested the ability of DGJ to rescue α-Gal A activity in the mutants. Each *GLA* variant analysed caused a deficiency of α-Gal A when expressed in COS-1 cells (Table 2, Fig. 3A), suggesting that all of them have a functional deleterious effect. Four variants: c.400T > C p.(Tyr134His), c.680G > C p.(Arg227Pro), c.815A > T p.(Asn272Ile) and c.1163_1165delTCC p.(Leu388del) caused complete absence of α-Gal A activity, severely affecting the protein function. DGJ did not increase the measured enzyme activity in these variants (Table 2, Fig. 3A). For the p.Tyr134His variant the DGJ increased the amount of detectable enzyme by western blot despite persistent absence of alpha-gal activity (Table 2, Fig. 3).

The two α-Gal A variants c.159C > G p.(Asn53Lys) and c.907A > T p.(Ile303Phe) caused partial α-Gal A deficiency with a residual activity of 46% and 14%, respectively, with respect to wild-type, (Table 1 and Fig. 3A). Incubation with 20 μM DGJ resulted in an increase of α-Gal A activity, by attaining maximum relative increases of 1.45 ± 0.21-fold ($n = 3$) (from 46 to 67% of wild-type) for c.159C > G p.(Asn53Lys) and 3.7 ± 0.16-fold ($n = 3$) (from 14% to 50% of wild-type) for c.907A > T p.(Ile303Phe) (Table 1). Mutant forms responsive to DGJ also showed an increase in α-Gal A protein levels after incubation with DGJ when analysed by western blot (Fig. 3B).

α-Gal A activity detected in non-transfected COS-1 cells was 115 ± 5.0 nmol/mg/h and this value was used to normalize α-Gal A activities measured in transfected COS-1 cells. α-Gal A activity of non-transfected COS-1 cells treated with 20 μM DGJ was 132 ± 5.0 nmol/mg/h.

3.7. Response to the DGJ on patients' derived lymphocytes

We tested the ability of the pharmacological chaperone DGJ to rescue the two mutant forms of α-Gal A p.Asn53Lys and p.Ile303Phe by administering DGJ directly to derived lymphocytes, in order to confirm

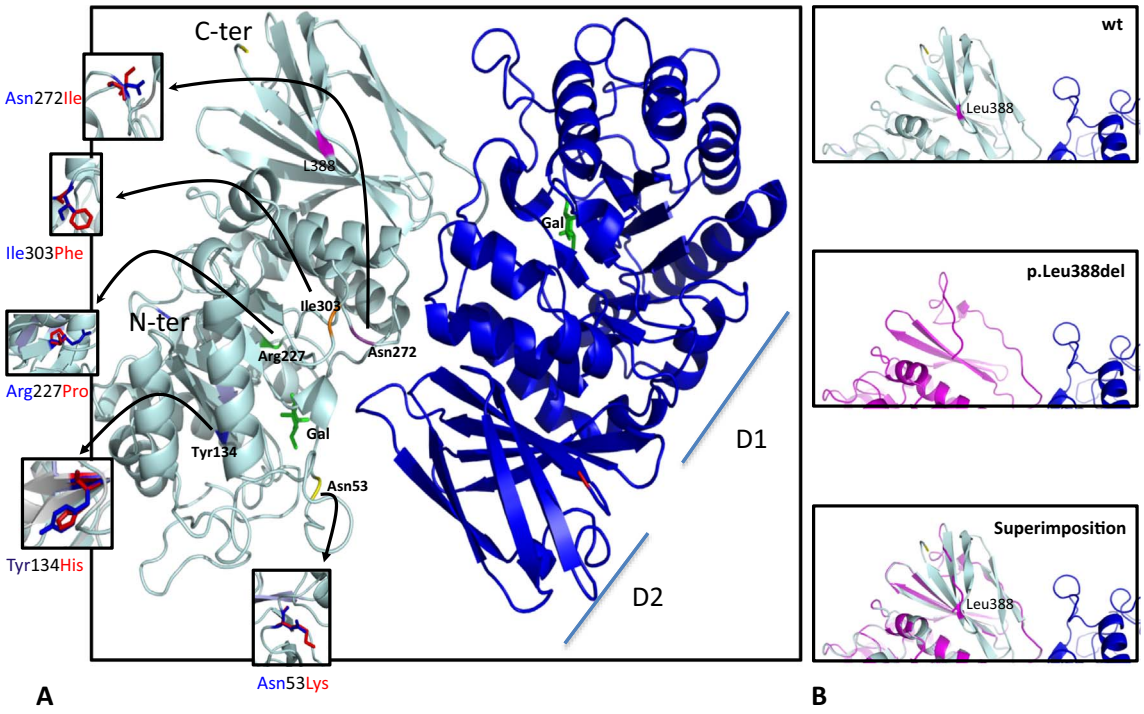

Fig. 2. Ribbon representation of the human α-Gal A and map of the studied variants localization obtained by homology modelling (HM) analysis. A) Ribbon representation of the human wild-type (wt) α-galactose-bounded α-Gal structure [27]. The two wt monomers are shown in dark-blue and light-blue. Each monomer is composed of two domains as pointed out for the dark-blue monomer: Domain 1 (D1) with the catalytic site, and Domain 2 (D2). Both the two D1 in this representation are bounded with an α-galactose molecule (green stick representation). The six residues involved in the studied variants are marked with different colours on the wt light-blue monomer. A zoom of the superimposed HM models obtained for each variants and the wt residue chain of interests is shown in the small windows (in blue the wt residues, while in red the mutated ones, all shown as sticks). B) In three different windows, from top to bottom, a zoom of the dramatic effect of missense mutation Leu388del is shown. In light blue the ribbon representation of the wt beta barrel that composes the D2 of the protein, in purple the Leu388del model obtained by HM. When the two structures are superimposed it is clear that such a substitution dramatically affects the integrity of the D2 of the protein. (For interpretation of the references to colour in this figure legend, the reader is referred to the web version of this article.)

what we observed *in vitro*.

In hemizygous p.Ile303Phe lymphocytes (established from Pt5) we found that DGJ improved α-Gal A enzyme activity by 17.5 times (Table 1). In heterozygous p.Asn53Lys lymphocyte (established from Pt1) the α-Gal A enzymatic activity (53 nmol/mg/h) fell within the normal range (> 20 nmol/mg/h), which made it impossible to determine to what extent, there was an increase in enzyme activity due to DGJ, if any. As FD is X-linked, cell populations derived from female patients contain a mixture of cells that express either wild-type or mutant α-Gal A. Hence, the baseline activity of the mutant form and the effect of DGJ on it can be difficult to accurately determine in heterozygous cell lines.

4. Discussion

Identifying of a novel *GLA* variant can leave confirmation of FD uncertain, particularly in patients harbouring missense variants and exhibiting mild manifestations or in female probands [4,6,7]. Functional and pharmacological studies of new *GLA* variants are necessary to understand their clinical significance and responsiveness to the chemical chaperone DGJ. An experimental strategy based on site-directed mutagenesis of the *GLA* cDNA and transient expression in mammalian cell models followed by α-Gal A enzyme assay and western blot analysis has proved effective in studying the extent of functional damage due to *GLA* variants [19,23,29,30]. This approach is also useful for investigating responsiveness of α-Gal A variants to chemical chaperones [19,23,29].

We used this strategy to study six *GLA* gene variants, c.159C > G p.(Asn53Lys), c.400T > C p.(Tyr134His), c.680G > C p.(Arg227Pro), c.815A > T p.(Asn272Ile), c.907A > T p.(Ile303Phe) and c.1163_1165delTCC p.(Leu388del).

4.1. The p.Tyr134His and p.Arg227Pro variants

The side-chain of p.Tyr134 and p.Arg227 amino acids occurs in the active site of human α-Gal A and interacts with the α-galactose

Table 2
Residual α-Gal A activities of mutant forms with and without DGJ in COS-1 cells.

Protein change	cDNA change	−DGJ		+DGJ		
		α-Gal A activity	% wt	α-Gal A activity	% wt	Relative increase
Wild-type	Wild-type	4822 ± 1147	100	4916 ± 1324	102	–
Asn53Lys	c.159C > G	2220 ± 119	46	3241 ± 641	67	1.45 ± 0.21
Tyr134His	c.400T > C	0.0 ± 0.0	0.0	17 ± 13	0.3	–
Arg227Pro	c.680G > C	0.0 ± 0.0	0.0	0.0 ± 0.0	0.0	–
Asn272Ile	c.815A > T	0.0 ± 0.0	0.0	0.0 ± 0.0	0.0	–
Ile303Phe	c.907A > T	664 ± 101	14	2441 ± 270	50	3.7 ± 0.16
Leu388del	c.1163_1165delTCC	0.0 ± 0.0	0.0	0.0 ± 0.0	0.0	–

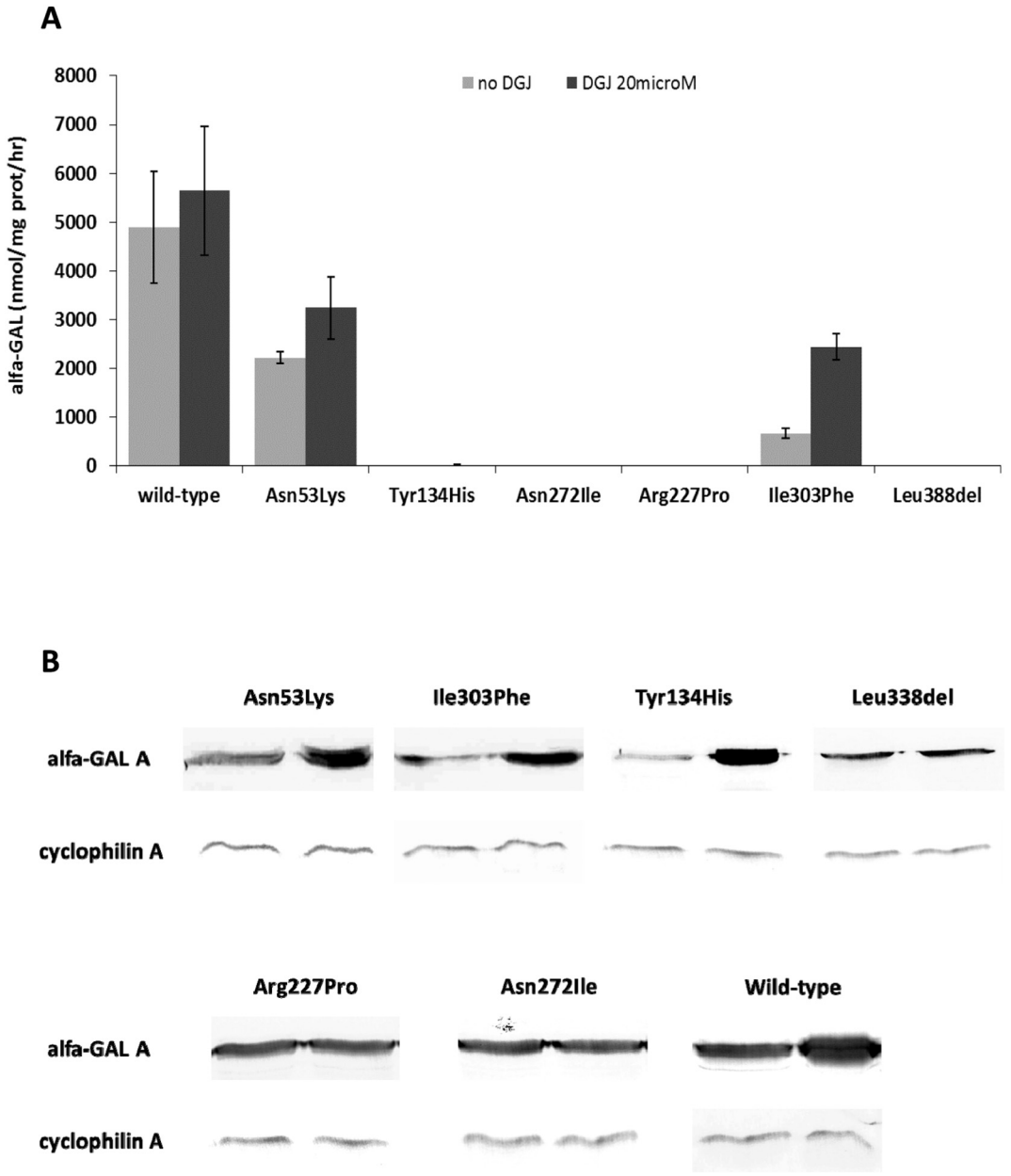

Fig. 3. α-Gal A enzyme activity and western blot analysis of COS-1 cells transfected with wild-type *GLA* cDNA and mutant forms, incubated with and without DGJ. A) α-Gal A activities are expressed as nmol 4-MU released/mg-protein/h in lysates from transfected COS-1 cells. Bars represent mean ± SD of at least three independent experiments. Mutant forms with no associated bar did not have any quantifiable baseline α-Gal A activity nor a response to DGJ. The data have been normalized to the α-Gal A activity of untreated COS-1 cells (115 nmol/mg/h with and 132 nmol/mg/h with 20 μM DGJ). B) COS-1 cells transiently transfected with the indicated wild-type and mutant forms of *GLA* cDNA were incubated for 48 h without (light grey bars) or with 20 μM DGJ (dark grey bars). Blots were conducted using 30 μg total protein, the anti-α-Gal-A antibody, and an anti-cyclophilin A antibody as a loading control (see Materials and Methods). The data for each mutant form are representative of at least three independent experiments with similar results.

substrate [26]. Both p.Tyr134 and p.Arg227 are extremely conserved in the phylogeny of the α-Gal A protein [26]. When expressed, the p.Tyr134His and p.Arg227Pro substitutions cause total loss of enzyme activity and reduction of enzyme protein expression (Fig. 3A). 20 μM DGJ increased the protein levels of the p.Tyr134His variant (Fig. 3B), unfortunately with no rescue of enzyme activity (Fig. 3A). Such findings, taken together with the clinical history of Pt2 and Pt3 (Table 1), suggest that the p.Tyr134His and p.Arg227Pro variants, both affecting the active site, correlate with classic FD. Two other substitutions, one affecting the p.Tyr134 residue, resulting in the polar amino acid serine p.(Tyr134Ser) [31], and one affecting the p.Arg227 residue, resulting in the polar amino acid glutamine p.(Arg227Gln) [32] have previously been reported and linked to classic FD [31,32].

4.2. The p.Asn272Ile variant

The p.Asn272Ile variant leads to the substitution of a polar with a non-polar residue. The side-chain of p.Asn272 occurs in a buried site not involved in the active site of human α-Gal A [26]. The p.Asn272 residue is highly conserved in the phylogeny of α-Gal A up to the Southern house mosquito, *Culex quinquefasciatus* (Alamut output, see Materials and Methods section). When expressed, the p.Asn272Ile amino acid substitution causes total deficiency of α-Gal A enzyme activity (Fig. 3A). DGJ did not rescue protein expression (Fig. 3B) or enzyme activity (Fig. 3A). We identified this variant in a female patient with a history of acroparesthesias (Pt4) who exhibited mild myocardial hypertrophy and proteinuria. Two other substitutions affecting the p.Asn272 codon have previously been reported in FD [33,34]: one

Table 3
α-Gal A enzyme activities of primary T-lymphocyte cultures from Pt1 (p.Asn53Lys) and Pt5 (p.Ile3030Phe) incubated with DGJ (normal > 20 nmol/mg/h).

Protein change	cDNA change	α-Gal A activity		Relative increase
		−DGJ	+DGJ	
Wild-type	Wild-type	40.7 ± 9.4	54.5 ± 10.5	1.3 ± 0.1
Asn53Lys	c.159C > G	53.0 ± 3.2	65.2 ± 6.3	1.2 ± 0.1
Ile303Phe	c.907A > T	1.2 ± 0.3	20.3 ± 2.3	17.5 ± 3.5

resulting in the polar amino acid lysine (p.Asn272Lys) [33] and one resulting in the polar amino acid serine (p.Asn272Ser) [34]. HM analysis of the protein revealed no conformational change, due to its loop region localization. A more careful look at 3-D Asn272 localization revealed that this residue is localized beyond the well-conserved Phe273 residue, essential for protein dimerization in different species. Such a localization of the Asn272 could then have an impact on the protein structure, due to hydrogen bond rearrangements in the p.Asn272Ile substitution. We tried to verify this hypothesis by performing some western blot analysis in non-denaturing conditions, but these experiments did not produce convincing results (data not shown), therefore this inference remains untested.

4.3. The p.Leu388del variant

The p.Leu388del variant causes the in-frame ablation of a single amino acid residue. The p.Leu388 residue is not involved in the α-Gal A active site [26]. It is highly conserved in the phylogeny up to Atlantic salmon, *Salmo salar* (Alamut output, see Materials and Methods section). HM analysis shows a severe structural effect of the p.Leu388del on the α-Gal A structure. In this study, the p.Leu388del is the only variant affecting the D2 domain of the protein. This single-amino acid deletion causes the loss of three antiparallel beta strands (beta 14, beta 15 and beta 16) resulting in a destruction of the D2 domain and misfolding of the last C-terminal forty-one residues (Fig. 2B). The modelling results suggest that the last three strands unfold, but deletion mutations could also introduce more local changes in the protein as happens for the most common CFTR mutation, Phe508del, which leads to less efficient folding of the protein, but the protein that does fold is functional [35]. Given the location of the Leu388del mutation at the end of a beta strand, it is also possible that the deletion is accommodated by a shorter beta turn and some local rearrangements. The cellular assay showed that protein is made but is not active (Fig. 3A). The p.Leu388del caused complete deficiency of α-Gal A activity and did not respond to DGJ (Fig. 3). We identified this deletion in the youngest patient (Pt6, 11 years old) of our cohort. He presented with clinical manifestations consistent with early onset FD (Table 1), including abdominal pain, diarrhea and recurrent fever. Such functional and clinical findings suggest that the p.Leu388del α-Gal A mutation correlates with classic FD.

4.4. The p.Asn53Lys variant

The p.Asn53Lys variant leads to a substitution with moderate physiochemical differences between neutral asparagine and basic lysine. The side-chain of p.Asn53 is localized in a loop region exposed at the surface of the protein that is not involved in the active site of human α-Gal A (Fig. 2). p.Asn53 is moderately conserved in the phylogeny of α-Gal A (Alamut output, see Materials and Methods section). Our results showed that the p.Asn53Lys amino acid substitution yields 46% of residual enzyme activity (Table 2, Fig. 3A). DGJ increased enzyme activity by 1.45 ± 0.21 times to 67% of the wild-type (Table 2, Fig. 3A) and also increased α-Gal A protein levels (Fig. 3B). Such results suggests that the p.Asn53Lys variant could correlate with a mild form of FD. We identified this variant in a female patient (Pt1) who exhibited isolated renal involvement starting by the age of 43 years. We also performed a renal biopsy in the patient. The histological analysis detected zebra bodies, the typical intracellular inclusions (data not shown). Another substitution affecting the p.Asn53 amino acid but resulting in polar aspartic acid, the p.Asn53Asp variant, has been reported in a female, but a detailed clinical description was not given [36].

4.5. The p.Ile303Phe variant

The p.Ile303Phe variant substitutes an aliphatic with an aromatic side chain. The side-chain of p.Ile303 occurs in a partially buried hydrophobic pocket not involved in the active site of human α-Gal A [26]. The p.Ile303 is phylogenetically highly conserved up to Atlantic salmon, *Salmo salar* (Alamut output, see Materials and Methods section). Another substitution affecting the p.Ile303 amino acid residue but resulting in polar neutral asparagine (p.Ile303Asn) has been reported and associated with classic FD [37]. The p.Ile303Phe substitution resulted in residual enzyme activity both when expressed and when measured on male patient's lymphocytes (Tables 1 and 3). Administration of DGJ to the expressed p.Ile303Phe increased α-Gal A enzyme activity by 3.7 ± 0.16 fold to 50% of the wild-type (Table 2). The administration of DGJ to patient's derived lymphocytes increased the α-Gal A enzyme activity by 17.5 times giving a value as high as in normal controls (20.3 ± 2.3 nmol/mg/h; normal > 20 nmol/mg/h) (Table 3). We identified the p.Ile303Phe variant in a male patient (Pt5; Table 1) who exhibited isolated hypertrophic cardiomyopathy at the age of 34 years and high lyso-Gb3 in plasma (23,6 ng/ml; normal < 0.8 ng/ml). Such functional and clinical findings suggest that the p.Ile303Phe α-Gal A mutation correlates with a mild variant of FD, which is suitable for treatment with DGJ.

Summarizing, we identified four severe *GLA* mutations: c.400T > C p.(Tyr134His), c.680G > C p.(Arg227Pro), c.815A > T p.(Asn272Ile) and c.1163_1165delTCC p.(Leu388del) and two mild variants: c.159C > G p.(Asn53Lys) and c.907A > T p.(Ile303Phe) partially responsive to the pharmacological chaperone DGJ.

5. Conclusions

5.1. Take-home message

Many patients who suffer FD achieve the diagnosis after an "odyssey" of tests and clinical evaluations. For this reason, when a *GLA* VUS is discovered in a suspected or confirmed FD patient, functional and pharmacological studies should be mandatory so that its clinical relevance and responsiveness to pharmacological chaperone therapy can be better understood. When functional data regarding a given *GLA* VUS are available but inconclusive and a diagnosis of FD remains plausible (as in case of patient 1), it is advisable to proceed with further medical investigations (*i.e.* tissue biopsy). It is important to shed light on the clinical significance of a *GLA* VUS to avoid inappropriate counselling and unnecessary and expensive treatment, particularly in this era of emerging newborn screening programs for lysosomal storage disorders that often result in the identification of genetic variants in asymptomatic infants.

Conflict of interests

Nothing to declare.

Acknowledgements

The authors wish to express their gratitude to AMMeC ONLUS (Associazione Malattie Metaboliche Congenite, Italia) for offering assistance in computer repairs.

Funding

This work was supported by the Italian Ministry of Health (grant

Ricerca Finalizzata RF-2011-02347694); the Fondazione Meyer ONLUS, Firenze, Italia (Meyer Children's Hospital's Young Researcher grant "Giovani Ricercatori-2a edizione"). The funders had no role in the design and conduct of the study; collection, management, analysis, and interpretation of the data; preparation, review, or approval of the manuscript; and decision to submit the manuscript for publication.

Ethics approval and consent to participate

Whole blood DNA samples from patients and their relatives were examined after informed consent was obtained for all individuals, in accordance with the Declaration of Helsinki and with local ethical committee recommendations.

Availability of data and material

The datasets used and/or analysed during the current study are available from the corresponding author upon reasonable request.

References

[1] R. Desnick, Y. Ioannou, C. Eng, α-Galactosidase A deficiency: Fabry disease, in: C.R. Scriver, A.L. Beaudet, W.S. Sly, D. Valle (Eds.), The metabolic and Molecular Bases of Inherited Disease, 8th ed., McGraw-Hill, New York, 2001, pp. 3733–3774.
[2] D.P. Germain, Fabry disease, Orphanet J. Rare Dis. 5 (2010) 30.
[3] L. Echevarria, K. Benistan, A. Toussaint, O. Dubourg, A.A. Hagege, D. Eladari, F. Jabbour, C. Beldjord, P. De Mazancourt, D.P. Germain, X-chromosome inactivation in female patients with Fabry disease, Clin. Genet. 89 (1) (2016) 44–54.
[4] S. Ferreira, A. Ortiz, D.P. Germain, M. Viana-Baptista, A. Caldeira-Gomes, M. Camprecios, M. Fenollar-Cortes, A. Gallegos-Villalobos, D. Garcia, J.A. Garcia-Robles, J. Egido, E. Gutierrez-Rivas, J.A. Herrero, S. Mas, R. Oancea, P. Peres, L.M. Salazar-Martin, J. Solera-Garcia, H. Alves, S.C. Garman, J.P. Oliveira, The alpha-galactosidase A p.Arg118Cys variant does not cause a Fabry disease phenotype: data from individual patients and family studies, Mol. Genet. Metab. 114 (2) (2015) 248–258.
[5] L. Ferri, C. Guido, G. la Marca, S. Malvagia, C. Cavicchi, A. Fiumara, R. Barone, R. Parini, D. Antuzzi, C. Feliciani, A. Zampetti, R. Manna, S. Giglio, C.M. Della Valle, X. Wu, K.J. Valenzano, R. Benjamin, M.A. Donati, R. Guerrini, M. Genuardi, A. Morrone, Fabry disease: polymorphic haplotypes and a novel missense mutation in the GLA gene, Clin. Genet. 81 (3) (2012) 224–233.
[6] R. Froissart, N. Guffon, M.T. Vanier, R.J. Desnick, I. Maire, Fabry disease: D313Y is an alpha-galactosidase A sequence variant that causes pseudodeficient activity in plasma, Mol. Genet. Metab. 80 (3) (2003) 307–314.
[7] M. Yasuda, J. Shabbeer, S.D. Benson, I. Maire, R.M. Burnett, R.J. Desnick, Fabry disease: characterization of alpha-galactosidase A double mutations and the D313Y plasma enzyme pseudodeficiency allele, Hum. Mutat. 22 (6) (2003) 486–492.
[8] G. Houge, C. Tondel, O. Kaarboe, A. Hirth, L. Bostad, E. Svarstad, Fabry or not Fabry–a question of ascertainment, Eur. J. Hum. Genet. 19 (11) (2011) 1111.
[9] B.E. Smid, C.E. Hollak, B.J. Poorthuis, M.A. van den Bergh Weerman, S. Florquin, W.E. Kok, R.H. Lekanne Deprez, J. Timmermans, G.E. Linthorst, Diagnostic dilemmas in Fabry disease: a case series study on GLA mutations of unknown clinical significance, Clin. Genet. 88 (2) (2015) 161–166.
[10] L. van der Tol, B.E. Smid, B.J. Poorthuis, M. Biegstraaten, R.H. Deprez, G.E. Linthorst, C.E. Hollak, A systematic review on screening for Fabry disease: prevalence of individuals with genetic variants of unknown significance, J. Med. Genet. 51 (1) (2014) 1–9.
[11] M. Lenders, F. Weidemann, C. Kurschat, S. Canaan-Kühl, T. Duning, J. Stypmann, B. Schmitz, S. Reiermann, J. Krämer, D. Blaschke, C. Wanner, S.M. Brand, E. Brand, Alpha-galactosidase A p.A143T, a non-Fabry disease-causing variant, Orphanet J. Rare Dis. 11 (1) (2016) 54.
[12] B.E. Smid, L. van der Tol, F. Cecchi, P.M. Elliott, D.A. Hughes, G.E. Linthorst, J. Timmermans, F. Weidemann, M.L. West, M. Biegstraaten, R.H. Lekanne Deprez, S. Florquin, P.G. Postema, B. Tomberli, A.C. van der Wal, M.A. van den Bergh Weerman, C.E. Hollak, Uncertain diagnosis of Fabry disease: consensus recommendation on diagnosis in adults with left ventricular hypertrophy and genetic variants of unknown significance, Int. J. Cardiol. 177 (2) (2014) 400–408.
[13] D.A. Hughes, K. Nicholls, S.P. Shankar, G. Sunder-Plassmann, D. Koeller, K. Nedd, G. Vockley, T. Hamazaki, R. Lachmann, T. Ohashi, I. Olivotto, N. Sakai, P. Deegan, D. Dimmock, F. Eyskens, D.P. Germain, O. Goker-Alpan, E. Hachulla, A. Jovanovic, C.M. Lourenco, I. Narita, M. Thomas, W.R. Wilcox, D.G. Bichet, R. Schiffmann, E. Ludington, C. Viereck, J. Kirk, J. Yu, F. Johnson, P. Boudes, E.R. Benjamin, D.J. Lockhart, C. Barlow, N. Skuban, J.P. Castelli, J. Barth, U. Feldt-Rasmussen, Oral pharmacological chaperone migalastat compared with enzyme replacement therapy in Fabry disease: 18-month results from the randomised phase III ATTRACT study, J. Med. Genet. 54 (4) (2017) 288–296.
[14] J.Q. Fan, S. Ishii, N. Asano, Y. Suzuki, Accelerated transport and maturation of lysosomal alpha-galactosidase A in Fabry lymphoblasts by an enzyme inhibitor, Nat. Med. 5 (1) (1999) 112–115.
[15] D.P. Germain, J.Q. Fan, Pharmacological chaperone therapy by active-site-specific chaperones in Fabry disease: in vitro and preclinical studies, Gene 47 (Suppl. 1) (2009) S111–7.
[16] D.P. Germain, D.A. Hughes, K. Nicholls, D.G. Bichet, R. Giugliani, W.R. Wilcox, C. Feliciani, S.P. Shankar, F. Ezgu, H. Amartino, D. Bratkovic, U. Feldt-Rasmussen, K. Nedd, U. Sharaf El Din, C.M. Lourenco, M. Banikazemi, J. Charrow, M. Dasouki, D. Finegold, P. Giraldo, O. Goker-Alpan, N. Longo, C.R. Scott, R. Torra, A. Tuffaha, A. Jovanovic, S. Waldek, S. Packman, E. Ludington, C. Viereck, J. Kirk, J. Yu, E.R. Benjamin, F. Johnson, D.J. Lockhart, N. Skuban, J. Castelli, J. Barth, C. Barlow, R. Schiffmann, Treatment of Fabry disease with the pharmacological chaperone migalastat, N. Engl. J. Med. 375 (2016) 545–555.
[17] R. Khanna, R. Soska, Y. Lun, J. Feng, M. Frascella, B. Young, N. Brignol, L. Pellegrino, S.A. Sitaraman, R.J. Desnick, E.R. Benjamin, D.J. Lockhart, K.J. Valenzano, The pharmacological chaperone 1-deoxygalactonojirimycin reduces tissue globotriaosylceramide levels in a mouse model of Fabry disease, Mol. Ther. 18 (1) (2010) 23–33.
[18] G.H. Yam, C. Zuber, J. Roth, A synthetic chaperone corrects the trafficking defect and disease phenotype in a protein misfolding disorder, FASEB J. 19 (1) (2005) 12–18.
[19] E.R. Benjamin, J.J. Flanagan, A. Schilling, H.H. Chang, L. Agarwal, E. Katz, X. Wu, C. Pine, B. Wustman, R.J. Desnick, D.J. Lockhart, K.J. Valenzano, The pharmacological chaperone 1-deoxygalactonojirimycin increases alpha-galactosidase A levels in Fabry patient cell lines, J. Inherit. Metab. Dis. 32 (3) (2009) 424–440.
[20] C. Filoni, A. Caciotti, L. Carraresi, M.A. Donati, R. Mignani, R. Parini, M. Filocamo, F. Soliani, L. Simi, R. Guerrini, E. Zammarchi, A. Morrone, Unbalanced GLA mRNAs ratio quantified by real-time PCR in Fabry patients' fibroblasts results in Fabry disease, Eur. J. Hum. Genet. 16 (11) (2008) 1311–1317.
[21] S. Ishii, S. Nakao, R. Minamikawa-Tachino, R.J. Desnick, J.Q. Fan, Alternative splicing in the alpha-galactosidase A gene: increased exon inclusion results in the Fabry cardiac phenotype, Am. J. Hum. Genet. 70 (4) (2002) 994–1002.
[22] L. Ferri, C. Cavicchi, A. Fiumara, R. Parini, R. Guerrini, A. Morrone, Pitfalls in the detection of gross gene rearrangements using MLPA in Fabry disease, Clin. Chim. Acta 452 (2015) 82–86.
[23] C. Filoni, A. Caciotti, L. Carraresi, C. Cavicchi, R. Parini, D. Antuzzi, A. Zampetti, S. Feriozzi, P. Poisetti, S.C. Garman, R. Guerrini, E. Zammarchi, M.A. Donati, A. Morrone, Functional studies of new GLA gene mutations leading to conformational Fabry disease, Biochim. Biophys. Acta 1802 (2) (2010) 247–252.
[24] S.H. Shin, S. Kluepfel-Stahl, A.M. Cooney, C.R. Kaneski, J.M. Quirk, R. Schiffmann, R.O. Brady, G.J. Murray, Prediction of response of mutated alpha-galactosidase A to a pharmacological chaperone, Pharmacogenet. Genomics 18 (9) (2008) 773–780.
[25] J.M. van Dongen, R. Willemsen, E.I. Ginns, H.J. Sips, J.M. Tager, J.A. Barranger, A.J. Reuser, The subcellular localization of soluble and membrane-bound lysosomal enzymes in I-cell fibroblasts: a comparative immunocytochemical study, Eur. J. Cell Biol. 39 (1) (1985) 179–189.
[26] S.C. Garman, D.N. Garboczi, The molecular defect leading to Fabry disease: structure of human alpha-galactosidase, J. Mol. Biol. 337 (2) (2004) 319–335.
[27] A.I. Guce, N.E. Clark, J.J. Rogich, S.C. Garman, The molecular basis of pharmacological chaperoning in human alpha-galactosidase, Chem. Biol. 18 (12) (2011) 1521–1526.
[28] C. Zizzo, I. Monte, A. Pisani, P. Fatuzzo, E. Riccio, M.S. Rodolico, P. Colomba, M. Uva, G. Cammarata, R. Alessandro, F. Iemolo, G. Duro, Molecular and clinical studies in five index cases with novel mutations in the GLA gene, Gene 578 (1) (2016) 100–104.
[29] J. Lukas, A.K. Giese, A. Markoff, U. Grittner, E. Kolodny, H. Mascher, K.J. Lackner, W. Meyer, P. Wree, V. Saviouk, A. Rolfs, Functional characterisation of alpha-galactosidase a mutations as a basis for a new classification system in fabry disease, PLoS Genet. 9 (8) (2013) e1003632.
[30] J. Shabbeer, M. Yasuda, S.D. Benson, R.J. Desnick, Fabry disease: identification of 50 novel alpha-galactosidase A mutations causing the classic phenotype and three-dimensional structural analysis of 29 missense mutations, Hum. Genomics 2 (5) (2006) 297–309.
[31] C.M. Eng, G.A. Ashley, T.S. Burgert, A.L. Enriquez, M. D'Souza, R.J. Desnick, Fabry disease: thirty-five mutations in the alpha-galactosidase A gene in patients with classic and variant phenotypes, Mol. Med. 3 (3) (1997) 174–182.
[32] C.M. Eng, L.A. Resnick-Silverman, D.J. Niehaus, K.H. Astrin, R.J. Desnick, Nature and frequency of mutations in the alpha-galactosidase A gene that cause Fabry disease, Am. J. Hum. Genet. 53 (6) (1993) 1186–1197.
[33] C.M. Eng, D.J. Niehaus, A.L. Enriquez, T.S. Burgert, M.D. Ludman, R.J. Desnick, Fabry disease: twenty-three mutations including sense and antisense CpG alterations and identification of a deletional hot-spot in the alpha-galactosidase A gene, Hum. Mol. Genet. 3 (10) (1994) 1795–1799.
[34] F. Verovnik, D. Benko, B. Vujkovac, G.E. Linthorst, Remarkable variability in renal disease in a large Slovenian family with Fabry disease, Eur. J. Hum. Genet. 12 (8) (2004) 678–681.
[35] G.L. Lukacs, A.S. Verkman, CFTR: folding, misfolding and correcting the DeltaF508 conformational defect, Trends Mol. Med. 18 (2) (2012) 81–91.
[36] C.L. Tai, M.Y. Liu, H.C. Yu, C.C. Chiang, H. Chiang, J.H. Suen, S.M. Kao, Y.H. Huang, T.J. Wu, C.F. Yang, F.C. Tsai, C.Y. Lin, J.G. Chang, H.D. Chen, D.M. Niu, The use of high resolution melting analysis to detect Fabry mutations in heterozygous females via dry bloodspots, Clin. Chim. Acta 413 (3–4) (2012) 422–427.
[37] J. Shabbeer, M. Yasuda, E. Luca, R.J. Desnick, Fabry disease: 45 novel mutations in the alpha-galactosidase A gene causing the classical phenotype, Mol. Genet. Metab. 76 (1) (2002) 23–30.